Electrooxidation of the iodides [C(4)mim]I, LiI, NaI, KI, RbI, and CsI in the room temperature ionic liquid [C(4)mim][NTf2]

ARTICLE *in* THE JOURNAL OF PHYSICAL CHEMISTRY C · APRIL 2008

Impact Factor: 4.77 · DOI: 10.1021/jp800145k

5 AUTHORS, INCLUDING:

Debbie S. Silvester
Curtin University
55 PUBLICATIONS **1,681** CITATIONS
SEE PROFILE

Leigh Aldous
University of New South Wales
89 PUBLICATIONS **1,834** CITATIONS
SEE PROFILE

Electrooxidation of the Iodides [C_4mim]I, LiI, NaI, KI, RbI, and CsI in the Room Temperature Ionic Liquid [C_4mim][NTf_2]

Emma I. Rogers,[†] Debbie S. Silvester,[†] Leigh Aldous,[‡] Christopher Hardacre,[‡] and Richard G. Compton*,[†]

Physical and Theoretical Chemistry Laboratory, Oxford University, South Parks Road, Oxford OX1 3QZ, United Kingdom, and School of Chemistry and Chemical Engineering/QUILL, Queen's University Belfast, Belfast, Northern Ireland BT9 5AG, United Kingdom

Received: January 8, 2008; In Final Form: February 13, 2008

The electrochemical oxidation of 1-butyl-3-methylimidazolium iodide, [C_4mim]I, has been investigated by cyclic voltammetry at a platinum microelectrode at varying concentrations in the RTIL 1-butyl-3-methylimidazolium bis(trifluoromethylsulfonyl)imide, [C_4mim][NTf_2]. Two oxidation peaks were observed. The first peak is assigned to the oxidation of iodide to triiodide, in an overall two-electron process: $3I^- - 2e^- \rightarrow I_3^-$. At higher potentials, the electrogenerated triiodide oxidizes to iodine, in an overall one-electron process: $I_3^- - e^- \rightarrow {}^3/_2I_2$. An average diffusion coefficient, D, for I^- of 1.55×10^{-11} m^2 s^{-1} was obtained. A digital simulation program was used to simulate the voltammetric response, and kinetic parameters were successfully extracted. The parameters deduced from the simulation include D for I^-, I_3^-, and I_2 and $K_{eq,2}$, the equilibrium constant for the reaction of iodide and iodine to form triiodide. Values for these parameters are of the same order as those previously published for the oxidation of Br^- in the same RTIL [Allen et al. *J. Electroanal. Chem.* **2005**, *575*, 311]. Next, the cyclic voltammetry of five different inorganic iodide salts was studied by dissolving small amounts of the solid in [C_4mim][NTf_2]. Similar oxidation peaks were observed, revealing diffusion coefficients of ca. 0.55, 1.14, 1.23, 1.44, and 1.33×10^{-11} m^2 s^{-1} and solubilities of 714, 246, 54, 83, and 36 mM for LiI, NaI, KI, RbI, and CsI, respectively. The slightly smaller diffusion coefficients for the XI salts (compared to [C_4mim]I) may indicate that I^- is ion-paired with Li^+, Na^+, K^+, Rb^+, and Cs^+ in the RTIL medium.

1. Introduction

Room temperature ionic liquids (RTILs) are salts that are comprised entirely of ions, generally a bulky, asymmetric organic cation and a weakly coordinating inorganic/organic anion, that exist in the liquid phase around room temperature, ca. 298 K.[1,2] The ability to vary the cation and anion combination allows properties that are tailored to suit the application of interest, and RTILs can therefore be described as "designer solvents''.[3] As solvents they are often considered "greener" for the environment compared with volatile organic compounds (VOCs) due to their negligible volatility (low vapor pressure);[1,3] however, their toxicity is likely to be no less than that of the component ions. Other properties they typically possess include high chemical and thermal stability, high viscosity (giving diffusion coefficients generally 1−2 orders of magnitude smaller than in traditional solvents), and low combustibility.[1,2] Their wide electrochemical potential windows allow them to be usefully employed as supporting electrolytes in a range of conventional solvents, e.g., acetonitrile.[1,2,4] In addition, the intrinsic conductivity of ionic liquids means that the use of a supporting electrolyte is not necessary when employing RTILs as electrochemical solvents, thus simplifying experimental setup and reducing waste.[1,2,4,5]

Ionic liquids have recently been applied in organic synthesis and catalysis, in synthesis of nanomaterials, and as electrolytes in numerous electrochemical devices, such as electric double-layer capacitors, fuel cells, actuators, lithium batteries, and dye-sensitized solar cells (DSSCs).[6−8] In DSSCs, the electrolyte contains a redox couple, which plays a role both in charge transfer and in the reduction of the photooxidized dye molecule.[6,7,9] The most promising redox couple so far is the iodide|triiodide ($I^-|I_3^-$) system,[6−10] as it is stable and reversible,[9] and has led to development of highly efficient solar cells.[8]

Commonly, ionic liquids are synthesized in a two-step process.[11] The first step is the alkylation of an amine, e.g., pyridine, etc., using a haloalkane to form an organic halide salt cation. The second step is the conversion of this halide salt via a metathesis reaction, either by replacement of the halide by an alkali metal salt or by addition of an acid to initiate anion exchange (for metathesis reaction scheme of an imidazolium RTIL, see Figure 1). The halide is removed by washing with water or dichloromethane, although obtaining a halide-free ionic liquid using this method is difficult.[11,12]

It is therefore important to quantify the amount of halide present in a sample[13] since various physical properties of the resulting RTILs are strongly influenced by the presence of halide impurities, even in small concentrations. For example, the viscosity of the liquid has been shown to increase dramatically with increasing concentration of chloride impurity,[14] and the electrochemical window of the ionic liquid was shown to narrow substantially with increasing halide presence.[1,2] The quantification of halides by simple and accurate methodology would be advantageous. To date, there have been numerous methods to determine halide concentration, including spectrophotometric,[15]

* Corresponding author. E-mail: richard.compton@chem.ox.ac.uk. Tel: +44(0) 1865 275 413. Fax: +44(0) 1865 275 410.
[†] Oxford University.
[‡] Queen's University Belfast.

10.1021/jp800145k CCC: $40.75
Published on Web 03/25/2008

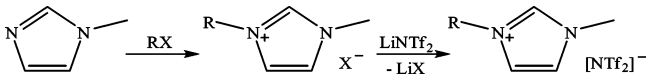

Figure 1. Reaction mechanism for the preparation of an imidazolium RTIL.[11]

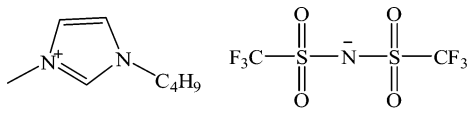

$[C_4mim]^+$ $[NTf_2]^-$

Figure 2. Structures of the cation and anion used as the RTIL in this study.

spectroscopic,[16] chromatographic,[17,18] spectroelectrochemical,[19] and, more recently, voltammetric methods.[12,20−23] The mechanistic aspects of halide oxidation (in aqueous solution) have also been studied thoroughly by pulse radiolysis techniques, and spectroscopic analysis of the intermediates of these reactions has allowed kinetic parameters to be deduced.[25,26]

The electrochemical oxidation mechanisms of iodide (I^-), bromide (Br^-), and chloride (Cl^-), collectively called the halides (X^-), have been studied in both conventional solvents and RTIL media using voltammetric methods. Kolthoff and Coetzee[27] investigated the electrooxidation of I^-, Br^-, and Cl^- in acetonitrile and observed two oxidation waves, which they assigned to the formation of the trihalide (X_3^-), followed by the formation of the halogen (X_2), shown in eqs 1 and 2.

$$3X^- - 2e^- \rightarrow X_3^- \quad (1)$$

$$X_3^- - e^- \rightarrow \frac{3}{2}X_2 \quad (2)$$

This mechanism is analogous to that obtained for the oxidation of iodide in acetonitrile[27−29] and in $[C_4mim][BF_4]$,[24,30] for the oxidation of chloride in $[C_4mim][BF_4]$,[12] $[C_4mim][NTf_2]$,[12,31] $[C_4mim][PF_6]$,[12] and $[C_4mpyrr][NTf_2]$,[21] and for the oxidation of bromide in acetonitrile,[22,23] $[C_4mim][NTf_2]$[22,23] and $[C_4mpyrr][NTf_2]$.[32] (Here, $[C_4mim]^+$ = 1-butyl-3-methylimidazolium, $[BF_4]^-$ = tetrafluoroborate, $[NTf_2]^-$ = bis(trifluoromethylsulfonyl)imide, $[PF_6]^-$ = hexafluorophosphate, and $[C_4mpyrr]^+$ = *N*-butyl-*N*-methylpyrrolidinium.)

Allen et al.[23] recently undertook a detailed investigation into the oxidation of $[C_2mim]Br$ in $[C_4mim][NTf_2]$ to deduce the various kinetic parameters. The voltammetric response was successfully modeled, using the simulation software DigiSim 3.03 (BAS Technicol),[33] following the mechanism above, involving the heterogeneous oxidation of halide to trihalide, denoted by eq 1, followed by the dissociation of trihalide to halogen, shown in eq 2.

Herein we aim to undertake a similar detailed investigation of the electrooxidation of iodide, sourced from several inorganic iodide salts, namely sodium iodide, lithium iodide, potassium iodide, rubidium iodide, and cesium iodide, as well as the iodide ionic liquid, $[C_4mim]I$, in the room temperature ionic liquid 1-butyl-3-methylimidazolium bis(trifluoromethylsulfonyl)imide, $[C_4mim][NTf_2]$ (see Figure 2). Then, we will use the voltammetry otained to extract kinetic parameters for the iodide oxidation process using digital simulation.

2. Experimental Section

2.1. Chemical Reagents. Lithium iodide, sodium iodide, potassium iodide, cesium iodide, rubidium iodide (Sigma-Aldrich, 99%), acetonitrile (Fischer Scientific, dried and distilled, >99%), and tetra-*n*-butylammonium perchlorate (TBAP, Fluka, Puriss electrochemical grade, >99%) were used as received without further purification. 1-Butyl-3-methylimidazolium bis(trifluoromethylsulfonyl)imide, $[C_4mim][NTf_2]$, was prepared by standard literature procedures.[11,34] 1-Butyl-3-methylimidazolium iodide was prepared as detailed in the literature.[11]

2.2. Instruments. A computer-controlled μ-Autolab potentiostat (Eco-Chemie, Netherlands) was used to perform all electrochemical experiments. A conventional two-electrode arrangement was utilized to study the voltammetry of all species, consisting of a platinum working electrode (10 μm diameter) and a silver quasi-reference electrode (0.5 mm diameter). A small section of disposable pipet tip was used to modify the microelectrode and form a small cavity above the electrode surface into which the RTIL solvent is placed in microlitre quantities (typically 20 μL). The electrodes were housed in a specially designed "T-cell'' (reported previously),[21,35] which allows study of ionic liquids under a controlled atmosphere. All experiments were undertaken in a heated Faraday cage (298 ± 1 K), which also served to minimize background noise. All solutions were purged under vacuum for at least 90 min prior to any measurements and for the duration of the experiment.

Saturated solutions of LiI, NaI, KI, RbI, and CsI were made up directly in 60 μL of $[C_4mim][NTf_2]$, which had previously been purged for 2 h under vacuum (0.05 Torr). The solutions were then stirred for ca. 12 h in foil-covered, sealed vials (to protect from light and moisture). 20 μL of this solution was then placed in the T-cell, and the electrochemical analysis was undertaken. Solutions of $[C_4mim]I$ at varying concentrations were made up directly in the T-cell by adding varying volumes of $[C_4mim]I$ to $[C_4mim][NTf_2]$ to give approximate concentrations of 50, 20, 9, 5, 3.3, 2.5, 1, 0.5, 0.25, and 0.125 vol %.

Prior to the analysis of each solution, the microdisk electrode was polished using 1 and 0.3 μm water−alumina (Buehler, Lake Bluff, IL) slurry on soft lapping pads (Kemet Ltd., Kent, U.K.). The electrode was calibrated to give the electrode diameter by analyzing the steady-state voltammetry of a 2 mM solution of ferrocene, containing 0.1 M TBAP, adopting a value for D of ferrocene in MeCN of 2.3×10^{-9} m^2 s^{-1}.[36]

2.3. Double Potential Step Chronoamperometric Experiments. Potential step chronoamperometric transients were achieved using a sample time of 0.01 s. The solution was pretreated by holding the potential at a point corresponding to zero faradaic current for 20 s, after which the potential was stepped to a position after the peak, and the current was measured for 10 s. The nonlinear curve fitting function, as proposed by Shoup and Szabo[37] for the time-dependent current response at microdisk electrodes, in the software package Origin-Pro 7.5 (Microcal Software Inc.) was employed to extract diffusion coefficient and solubility data from these transients. The equations used in this approximation are shown below and sufficiently describe the current response to within 0.6% accuracy.

$$I = -4nFDcr_d f(\tau) \quad (3)$$

$$f(\tau) = 0.7854 + 0.8863\tau^{-1/2} + 0.2146\exp(-0.7823\tau^{-1/2}) \quad (4)$$

$$\tau = \frac{4Dt}{r_d^2} \quad (5)$$

where n is the number of electrons transferred, F is the Faraday constant, D is the diffusion coefficient, c is the initial concentration of parent species, r_d is the radius of the disk electrode, and

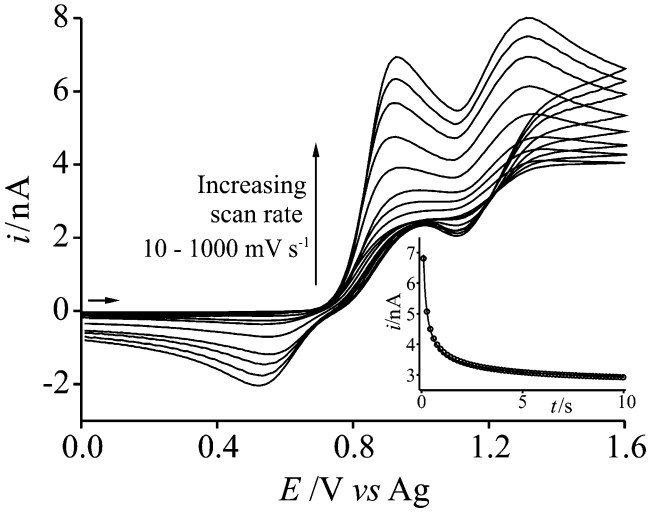

Figure 3. Cyclic voltammetry for the oxidation of 2.5 vol % [C$_4$mim]I in [C$_4$mim][NTf$_2$] on a platinum microelectrode (diameter 10 μm) at varying scan rates (10, 40, 80, 200, 400, 600, 800, and 1000 mV s^{-1}). The inset is the experimental (−) and fitted theoretical (○) chronoamperometric transient recorded for the oxidation of I^- . The potential was stepped from 0.0 to +1.1 V.

t is the time. 100 iterations were performed by the software, while fixing the value for the radius (determined previously by calibration) to give values for the diffusion coefficient (*D*) and a product of the number of electrons multiplied by the concentration (*nc*), after optimization of the experimental data.

3. Results and Discussion

The RTIL chosen in this study was [C$_4$mim][NTf$_2$] (see Figure 2 for structure), since this showed a wide electrochemical window, in excess of 4.5 V, and no measurable voltammetric features when fully purged under vacuum. The iodide salt of [C$_4$mim]$^+$ was also readily available.

3.1. Electrooxidation of [C$_4$mim]I in [C$_4$mim][NTf$_2$]. [C$_4$mim]I was chosen as a source of iodide ions as the anion can be studied independently without the countercation affecting the voltammetry obtained. The effect of concentration on the diffusion coefficient of iodide was first investigated. Concentrations ranging from 50 to 0.125 vol % [C$_4$mim]I in [C$_4$mim][NTf$_2$] (7752−6 mM as determined by chronamperometry, see later) were studied on a 10 μm diameter platinum microelectrode at a range of scan rates. Figure 3 shows typical cyclic voltammetry for the oxidation of 2.5 vol. % (ca.140 mM) [C$_4$mim]I at scan rates from 10 to 1000 mV s^{-1}. The voltammetry gives rise to two well-defined, transient-shaped oxidation peaks at E_p = +0.93 and +1.21 V vs Ag, along with two corresponding reduction peaks at +0.52 and +1.10 V vs Ag, resulting from two-electrode processes. Similar voltammetric behavior has been observed previously for chloride, bromide, and iodide in the ionic liquids [C$_4$mim][PF$_6$], [C$_4$mim][BF$_4$], [C$_4$mpyrr][NTf$_2$], and [C$_4$mim][NTf$_2$].[12,22−24] It is likely that the same mechanism is taking place for the oxidation of iodide in this work; the first oxidation wave corresponds to the oxidation of iodide to molecular iodine, followed by the addition of iodide to form the triiodide anion, in an overall two-electron EC process[23] in which two-thirds of an electron is transferred per molecule of iodide transported to the electrode. This is summarized by eqs 6 and 7:

$$2I^- - 2e^- \rightarrow I_2 \quad (6)$$

$$I_2 + I^- \rightleftharpoons I_3^- \quad (7)$$

TABLE 1: Chronoamperometric Data[a] (*D* and *nc*) Using Shoup and Szabo[37] Approximations for Varying Concentrations of [C$_4$mim]I in [C$_4$mim][NTf$_2$], along with Values for *c* Calculated from *nc* Values (n = $^2/_3$) and from the Densities of the Two RTILs (labeled *c*′) at 298 K

[C$_4$mim]I/vol %	D_{I^-}/× 10^{-11} m^2 s^{-1}	*nc*/mM	*c*/mM	*c*′/mM
50	0.44 (±0.03)	5168 (±252)	7752	*b*
20	1.21 (±0.02)	834 (±12)	1251	*b*
9.1	1.53 (±0.02)	397 (±3.5)	596	*b*
5	1.09 (±0.02)	395 (±4.4)	593	*b*
3.33	1.27 (±0.02)	159 (±1.7)	239	*b*
2.5	1.41 (±0.13)	93 (±1.7)	140	144
1	1.54 (±0.03)	43 (±0.6)	65	56
0.5	1.70 (±0.06)	21 (±0.5)	32	28
0.25	1.60 (±0.05)	11 (±0.2)	17	14
0.13	1.51 (±0.08)	4 (±0.1)	6	7

[a] Error bars calculated from the standard deviation of the best theoretical fits from several repeat potential step chronoamperograms. [b] It is assumed that the volume change when mixing the two ionic liquids is zero; this assumption is not appropriate when mixing larger volumes of the more viscous ionic liquid, and so concentrations calculated from densities cannot be compared with concentrations determined from chronoamperometric techniques.

The second oxidation wave is assigned to the dissociation of electrogenerated triiodide to iodine and iodide (eq 8), followed by the formation of one iodine molecule for every two iodide anions (eq 9):

$$I_3^- \rightleftharpoons I_2 + I^- \quad (8)$$

$$I^- - e^- \rightarrow \frac{1}{2}I_2 \quad (9)$$

The overall reaction for both peaks is given by eq 10, where one electron is transferred per molecule of iodide.

$$3I^- - 3e^- \rightarrow \frac{3}{2}I_2 \quad (10)$$

From the shape of the peaks observed, the oxidation of iodide to triiodide appears to be an electrochemically irreversible process, with an increase in peak separation between oxidation and reduction peaks with increasing scan rate. This behavior corresponds well to that observed previously for both iodide and bromide in RTILs.[23,24]

In order to calculate diffusion coefficients, *D*, and concentrations, *c*, potential step chronoamperometry was performed on the first oxidative peak. The resulting transient (−) for the 140 mM solution is shown as an inset to Figure 3, along with the best theoretical fit (○) to the Shoup and Szabo[37] equation. This process was repeated for several concentrations. Table 1 summarizes all the data extracted from chronoamperometric analysis; *D* and *nc* values, where *n* is the number of electrons transferred ($^2/_3$ in this case) and solubility data, *c*, for iodide. Also shown in the table are the prepared concentrations (*c*′) calculated from the volume and density of [C$_4$mim]I in [C$_4$mim][NTf$_2$]. From the table, a small range in diffusion coefficients for the iodide anion ((0.44−1.70) × 10^{-11} m^2 s^{-1}) is observed from analysis of chronoamperometric transients. This likely arises as a result of the different viscosities of the two ionic liquids that make up the solution mixture (44 cP for [C$_4$mim][NTf$_2$][1] and 1110 cP for [C$_4$mim]I[38] at 298 K). No systematic trend was observed for the diffusion coefficient at varying concentrations, and so an average diffusion coefficient for the lower concentrations (0.13−2.5 vol %) of ca. (1.55 ± 0.11) × 10^{-11} m^2 s^{-1} for [C$_4$mim]I in [C$_4$mim][NTf$_2$] was

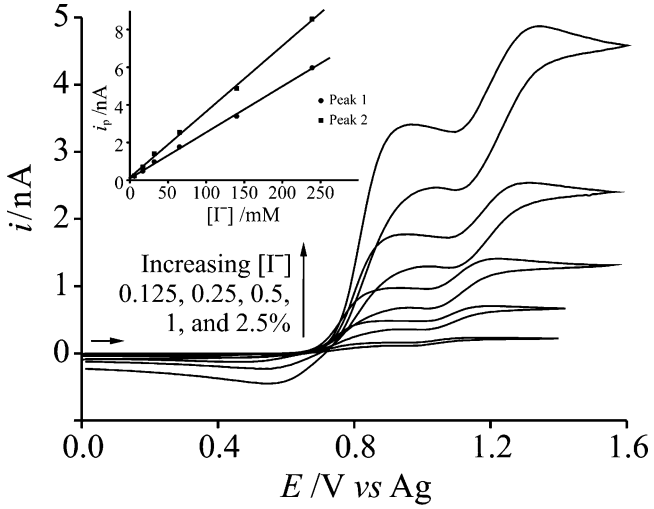

Figure 4. Cyclic voltammetry for the oxidation of $[C_4mim]I$ in $[C_4mim][NTf_2]$ on a platinum microelectrode (diameter 10 μm) at increasing concentrations (0.125, 0.25, 0.5, 1.0, and 2.5 vol %) at 100 mV s^{-1} . The inset to the figure shows a plot of peak current for both peaks vs iodide concentration (line of best: $R^2 = 0.99$ for both peaks).

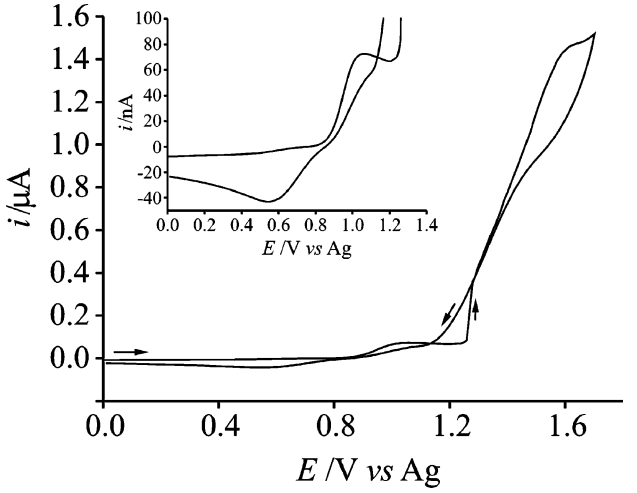

Figure 5. Cyclic voltammetry for the oxidation of 50 vol % $[C_4mim]I$ in $[C_4mim][NTf_2]$ on a platinum microelectrode (diameter 10 μm) at 100 mV s^{-1}. The inset to the figure shows a close-up view of peak 1, before the "nucleation loop''.

determined. This value is comparable in magnitude with that observed for the oxidation of $[C_4mim]I$ in $[C_4mim][BF_4]$ (2.00×10^{-11} m^2 s^{-1} at 295 K).[24]

Figure 4 shows typical cyclic voltammetry for the oxidation of iodide at concentrations of 0.125, 0.25, 0.5, 1.0, and 2.5 vol % (6−140 mM) $[C_4mim]I$ in $[C_4mim][NTf_2]$ at 100 mV s^{-1} on a 10 μm diameter Pt electrode. The peak current for all peaks increase consistently with increasing concentration. The inset to Figure 4 shows linear plots of peak current, i_p, vs iodide concentration, $[I^-]$, for both peaks, which implies that D is constant and therefore independent of concentration. The ratio of peak currents, i_{p1}/i_{p2}, is ca. 1.5 ± 0.1, which supports the mechanism assigned to the electrode processes occurring, where two-thirds of an electron is transferred in peak 1 and one-third of an electron is transferred in peak 2. This voltammetric behavior is observed for concentrations up to 2.5 vol % , above which a breakdown in the second peak is observed. For 3.33 vol % I^- (239 mM), two redox couples are observed; however, peak 2 becomes distorted and deviates from the behavior observed at lower concentrations. Above 239 mM, the second peak is no longer visible in the potential range under investigation. At much higher concentrations (7752 mM), a marked crossover, at ca. +1.20 V vs Ag, is observed between the forward and reverse scans of the second peak, characteristic of a "nucleation loop'',[39] after which a second oxidation peak is observed, ca. +1.63 V vs Ag, shown in Figure 5. It is possible that the presence of this loop and the shift of the second peak to a more positive potential is due to adsorption of iodide onto the silver wire quasi-reference. To investigate this, a platinum wire quasi-reference was utilized (replacing the silver wire) and the voltammetry of 50 vol % (7752 mM) $[C_4mim]I$ was investigated (voltammetry not shown). As with the silver wire, a nucleation loop was observed at +0.40 V vs Pt, with peak 2 at +0.91 V vs Pt, suggesting that it is not adsorption of iodide onto silver that causes the positive potential shift of the peak. Instead, the phenomenon is ascribed to the nucleation of iodine, i.e., a process in which iodine becomes deposited onto the platinum working electrode surface, which requires an activation energy to be provided by an overpotential.

3.2. Electrooxidation of Various Inorganic Iodide Salts in $[C_4mim][NTf_2]$. The voltammetric response of five different inorganic iodide salts (NaI, LiI, KI, RbI, and CsI) were next investigated at a 10 μm diameter platinum electrode in

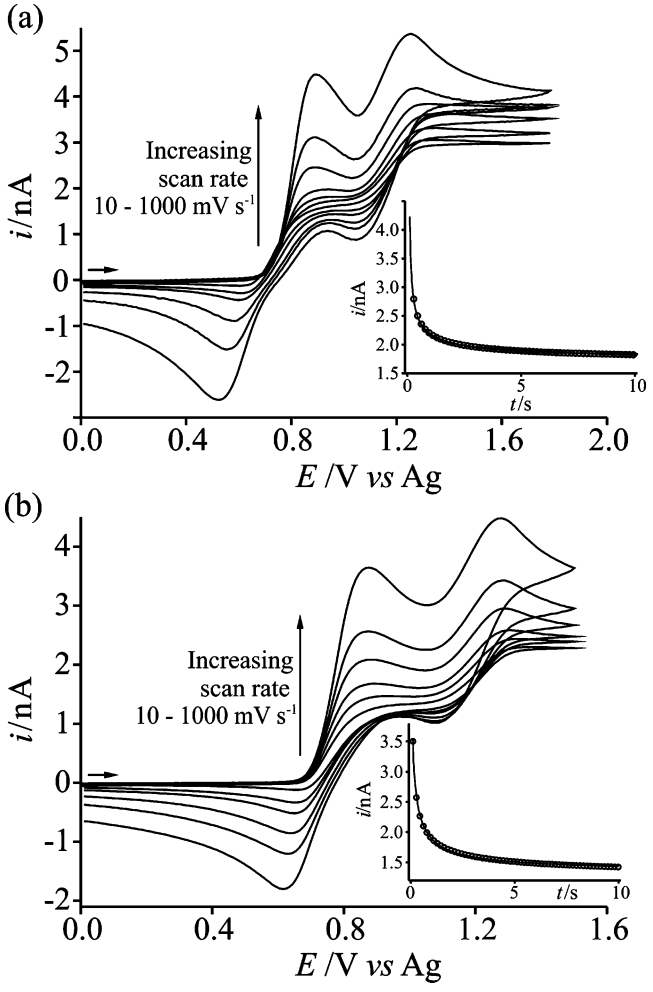

Figure 6. Cyclic voltammetry for the oxidation of (a) potassium iodide and (b) rubidium iodide in $[C_4mim][NTf_2]$ on a platinum microelectrode (diameter 10 μm) at varying scan rates (10, 40, 80, 200, 400, and 1000 mV s^{-1}). Inset to each is the experimental (−) and fitted theoretical (○) chronoamperometric transients recorded for the oxidation of I^- . The potential was stepped from 0.0 to +1.0 V.

TABLE 2: Chronoamperometric Data[a] (*D* and *nc*) Using Shoup and Szabo[37] Approximations for Five Different Inorganic Iodide Salts in [C_4mim][NTf_2], along with Values for *c* Calculated from *nc*, as $n = {}^2/_3$, at 298 K

iodide salt	$D_{I^-}/\times 10^{-11}$ m^2 s^{-1}	*nc*/mM	*c*/mM
LiI	0.55 (±0.01)	476 (±7.6)	714
NaI	1.14 (±0.02)	164 (±0.8)	246
KI	1.23 (±0.04)	36 (±1.4)	54
RbI	1.44 (±0.01)	55 (±0.6)	83
CsI	1.33 (±0.01)	24 (±0.1)	36

[a] Error bars calculated from the standard deviation of the best theoretical fits from several repeat potential step chronoamperograms.

[C_4mim][NTf_2]. Figure 6a,b shows typical cyclic voltammetry for the oxidation of saturated (ca. 54 and 83 mM) solutions of KI and RbI at scan rates from 10 to 1000 mV s^{-1}. Two waves are observed at $E_p = +0.90$ and $+1.30$ V vs Ag in both cases. Figure 1a−c in the Supporting Information shows similar cyclic voltammetry observed for NaI, LiI, and CsI. The same behavior is generally observed for all iodide salts. However, for NaI and LiI, peak 2 becomes distorted and deviates from observed behavior, possibly because the saturation point approaches the concentration limit where nucleation processes begin to occur (as explained in section 3.1). Peak currents recorded for the iodide salts studied are smaller (probably due to lower solubility) than the peak currents of [C_4mim]I in [C_4mim][NTf_2], despite the RTIL being saturated with XI, where $X^+ = Li^+$, Na^+, K^+, Rb^+, or Cs^+. Potential-step chronoamperometry was performed on the first oxidative peak of each iodide salt, and the resulting chronoamperometric transient (−) with the best theoretical fit (○) to the Shoup and Szabo[37] expression is shown as insets to Figure 6a,b for KI and RbI and as insets to Figure 1a−c in the Supporting Information for NaI, LiI, and CsI, respectively. The diffusion coefficients (*D*) and *nc* values obtained are summarized in Table 2 along with the solubility (*c*) of the iodide species, since *n* in this case equals ${}^2/_3$. The modest solubility of KI, RbI, and CsI (36−83 mM) may prove disadvantageous if this technique is to be applied to the analytical determination of these salts in RTILs. However, LiI and NaI are relatively quite soluble in the RTIL (714 and 246 mM, respectively), so there may be some scope for the analytical detection of these species in RTILs.

As mentioned in section 3.1, the average diffusion coefficient of [C_4mim]I in [C_4mim][NTf_2] is ca. 1.55×10^{-11} m^2 s^{-1}. The *D*'s of all the inorganic iodide salts were found to be slightly smaller than this value, suggesting the possibility of ion pairing between the iodide anion and X^+, leading to slower diffusion of XI through the RTIL. This phenomenon was observed previously for the diffusion coefficients of $NaNO_3$ and KNO_3 in RTILs.[40] The diffusion coefficients measured for all iodide salts are ca. 1−2 orders of magnitude smaller than in water[41] (1.62×10^{-9} and 2.00×10^{-9} m^2 s^{-1} for NaI and KI, respectively, at 298 K), in carbon tetrachloride[42] (4.2×10^{-9} m^2 s^{-1} for KI at 298 K), and NaCl melts[43] (2.68×10^{-10} m^2 s^{-1} for NaI at 448 K). This seems reasonable given the higher viscosity of the RTIL (44 cP)[1] compared to water (0.89 cP)[44] and tetrachloromethane (0.91 cP),[45] all at 298 K.

3.3. Modeling the Oxidation of Iodide in [C_4mim][NTf_2]. In order to extract kinetic data, the oxidation of [C_4mim]I in [C_4mim][NTf_2] was next simulated using the one-dimensional simulation program DigiSim 3.03 (BAS Technicol).[33] Scan rates ranging from 100 to 10 000 mV s^{-1} were simulated using the hemispherical diffusion model; the approximate validity of the latter has been assessed elsewhere.[46] It was found that that the two-step oxidation of iodide (from [C_4mim]I in this case) in

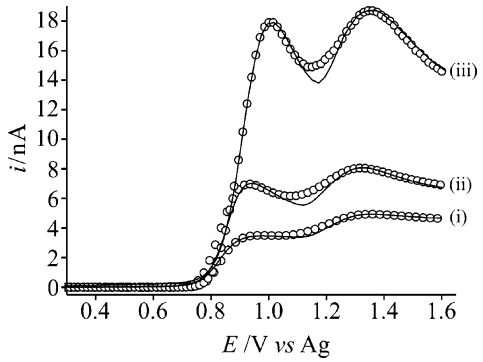

Figure 7. Comparison of the experimental (−) and simulated (○) cyclic voltammograms for the oxidation of 2.5 vol % [C_4mim]I in [C_4mim][NTf_2] at scan rates of (i) 100, (ii) 1000, and (iii) 10 000 mV s^{-1}, using values of *D* and *c* close to that obtained from chronoamperometric data. Parameters are given in Table 3.

TABLE 3: Parameters for I^- from the Simulation Fits for 1 and 2.5 vol % [C_4mim]I in [C_4mim][NTf_2]

parameter	1 vol % [C_4mim]I	2.5 vol % [C_4mim]I	[C_2mim]Br[a]
c/M	0.07 (±0.03)	0.14 (±0.003)	−
E_f^0/V	0.98 (±0.01)	1.01 (±0.01)	1.13
α^b	0.55	0.55	0.50
$k_0{}^{b,c}$/cm s^{-1}	0.01	0.01	0.006
$D_{I^-}/\times 10^{-11}$ m^2 s^{-1}	1.58 (±0.04)[d]	1.50 (±0.05)[d]	1.40
$D_{I_2}/\times 10^{-11}$ m^2 s^{-1}	4.50 (±0.50)[d]	4.90 (±1.00)[d]	2.00
$D_{I_3^-}/\times 10^{-11}$ m^2 s^{-1}	2.80 (±0.20)[d]	2.5 (±0.20)[d]	2.00
$K_{eq,2}$/mol^{-1} dm^3	8700	7500	ca. 3000

[a] Values published previously[23] for the oxidation of [C_4mim]Br in [C_4mim][NTf_2]. [b] These values were fixed in all simulations to give the best fit. [c] See text for a discussion indicating the absence of real physical significance for this quantity. [d] Diffusion coefficients were varied slightly to optimize the fits over a range of scan rates.

[C_4mim][NTf_2] could be successfully modeled following the reaction scheme:

$$3I^- - 2e^- \rightarrow I_3^- \quad (11)$$

$$I_3^- - e^- \rightarrow \frac{3}{2}I_2 \quad (12)$$

The simulation software requires that the mechanism is written as a series of single- or multielectron heterogeneous processes (described by Butler−Volmer kinetics), coupled with first or second homogeneous processes. For this reason, the mechanism is rearranged to "force fit'' the electrochemistry into the DigiSim conformity and to ensure the conversion of iodide to iodine with the kinetics observed. The generic mechanism entered into the program is as follows:

$$I^- - e^- \xrightarrow{k_0} I^\bullet \quad (13)$$

$$2I^\bullet \xrightarrow[k_{f,1}]{} I_2 \quad (14)$$

$$I^- + I_2 \underset{k_{b,2}}{\overset{k_{f,2}}{\rightleftharpoons}} I_3^- \quad (15)$$

where k_0 is the standard electrochemical rate constant, $k_{f,1}$ and $k_{f,2}$ are the rate constants of the dimerization of $I^\bullet$ and the formation of I_3^-, respectively, and $k_{b,2}$ is the rate constant of the dissociation of I_3^-. $K_{eq,1}$ is the "effective equilibrium constant'' for the fictitious reaction represented by eq 14 (which is needed to overcome the limitations of DigiSim) and is

calculated from the rate constant. $K_{eq,2}$ is the equilibrium constant for eq 15 and is calculated from the rate constants of the forward and backward reactions.

According to the following inequality[47]

$$v \ll \frac{RTD}{nFr_d^2} \tag{16}$$

where v is the scan rate, R is the universal gas constant, and T is the absolute temperature, and assuming the diffusion coefficient $D = 1.55 \times 10^{-11}$ m^2 s^{-1} (from electrochemical oxidation of [C_4mim]I, see section 3.1), $n = {}^2/_3$, and $r_d = 5.2$ μm, true steady-state behavior can only be achieved at scan rates much less than 21.9 mV s^{-1}. In this work, scan rates of 10−10 000 mV s^{-1} were explored.

Figure 7 shows the fits observed between the experimental (−) and theoretical (○) voltammograms for the oxidation of 2.5 vol % (ca. 140 mM) [C_4mim]I in [C_4mim][NTf_2] over a range of scan rates. As can be seen, excellent fits are observed between experimental and fitted theoretical data using the parameters given in Table 3. Values of α (charge-transfer coefficient) and k_0 were fixed as 0.55 and 0.01 cm s^{-1}. $K_{eq,1}$, $k_{f,1}$, and $k_{f,2}$ were chosen to be fictitiously large, and $D_{I^\bullet}$ (the diffusion coefficient of the fictitious I$^\bullet$ species) was chosen to be small. They were fixed as 1.00×10^{20} mol^{-1} dm^3, 1.00×10^{14} mol^{-1} dm^3 s^{-1}, 1.00×10^{14} mol^{-1} dm^3 s^{-1}, and 6.00×10^{-11} m^2 s^{-1}, respectively. Values for the parameters D_{I^-}, $D_{I_3^-}$, and D_{I_2} (diffusion coefficients of I^-, I_3^-, and I_2) were varied slightly (represented by the error bars quoted in the table) to optimize the simulation fits over a range of scan rates (100−10 000 mV s^{-1}). The rate constants $k_{f,1}$ and $k_{f,2}$ were arbitrarily selected and fictitiously large and beyond diffusion control to push the equilibrium over to promote the formation of I_2. $K_{eq,2}$ was found to vary between concentrations but was fixed over scan rates at individual concentrations. All the parameters used for the best fits to the experimental data are shown in Table 3. Also shown in the table are the parameters used for the simulation of Br^- in [C_4mim][NTf_2] in a different study.[23] Note, the values for k_0 have no physical meaning because of the fictitious nature of the I$^\bullet$ species introduced out of necessity due to the limitations of DigiSim.

4. Conclusions

The oxidation of 1-butyl-3-methylimidazolium iodide, [C_4mim]I, has been investigated by cyclic voltammetry at a platinum microelectrode in the RTIL 1-butyl-3-methylimidazolium bis(trifluoromethylsulfonyl)imide, [C_4mim][NTf_2]. Two oxidation peaks were observed and were assigned to the oxidation of iodide to triiodide, followed by the formation of iodine, in an overall one-electron process per iodide ion. A digital simulation program was used to simulate the voltammetric response, and kinetic parameters were successfully extracted, which were consistent with data published previously for Br^-. Next the cyclic voltammetry of five different inorganic iodide salts (LiI, NaI, KI, RbI, and CsI) was studied, and similar oxidation peaks were observed. Diffusion coefficients and solubilities were easily obtained for each iodide salt.

Acknowledgment. E.I.R. thanks the EPSRC, D.S.S. thanks Schlumberger Cambridge Research, and L.A. thanks the Department of Education and Learning in Northern Ireland and Merck GmBH for financial support.

Supporting Information Available: Figures showing cyclic voltammetry for the oxidation of sodium iodide, lithium iodide, and cesium iodide in [C_4mim][NTf_2] on a 10 μm diameter Pt electrode at increasing scan rates. This material is available free of charge via the Internet at http://pubs.acs.org.

References and Notes

(1) Buzzeo, M. C.; Evans, R. G.; Compton, R. G. *Chem. Phys. Chem.* **2004**, *5*, 1106−1120.
(2) Silvester, D. S.; Compton, R. G. *Z. Phys. Chem. (Munich)* **2006**, *220*, 1247−1274.
(3) Earle, M. J.; Seddon, K. R. *Pure Appl. Chem.* **2000**, *72*, 1391−1398.
(4) Endres, F.; Zein El Abedin, S. *Phys. Chem. Chem. Phys.* **2006**, *8*, 2101−2116.
(5) Hultgren, V. M.; Mariotti, A. W. A.; Bond, A. M.; Wedd, A. G. *Anal. Chem.* **2002**, *74*, 3151−3156.
(6) Takahashi, K.; Shingo, S.; Tezuka, H.; Hiejima, Y.; Katsumura, Y.; Watanabe, M. *J. Phys. Chem. B* **2007**, *111*, 4807−4811.
(7) Kawano, R.; Watanabe, M. *Chem. Commun.* **2005**, *16*, 2107−2109.
(8) Mazille, F.; Fei, Z.; Kuang, D.; Zhao, D.; Zakeeruddin, S. M.; Grätzel, M.; Dyson, P. J. *Inorg. Chem.* **2006**, *45*, 1585−1590.
(9) Paulsson, H.; Berggrund, M.; Svantesson, E.; Hagfeldt, A.; Kloo, L. *Sol. Energy Mater. Sol. Cells* **2004**, *82*, 345−360.
(10) Berginc, M.; Opara Krašovec, U.; Jankovec, M.; Topič, M. *Sol. Energy Mater. Sol. Cells* **2007**, *91*, 821−828.
(11) Bonhôte, P.; Dias, A.-P.; Papageorgiou, N.; Kalyanasundaram, K.; Grätzel, M. *Inorg. Chem.* **1996**, *35*, 1168−1178.
(12) Villagrán, C.; Banks, C. E.; Hardacre, C.; Compton, R. G. *Anal. Chem.* **2004**, *76*, 1998−2003.
(13) Wishart, J. F.; Castner, E. W. *J. Phys. Chem. B* **2007**, *111*, 4639−4640.
(14) Seddon, K. R.; Stark, A.; Torres, M.-J. *Pure Appl. Chem.* **2000**, *72*, 2275−2287.
(15) Anthony, J. L.; Maginn, E. J.; Brennecke, J. F. *J. Phys. Chem. B* **2001**, *105*, 10942−10949.
(16) Billard, I.; Moutiers, G.; Labet, A.; El Azzi, A.; Gaillard, C.; Mariet, C.; Lützenkirchen, K. *Inorg. Chem.* **2003**, *42*, 1726−1733.
(17) Villagrán, C.; Deetlefs, M.; Pitner, W. R.; Hardacre, C. *Anal. Chem.* **2004**, *76*, 2118−2123.
(18) Anderson, J. L.; Ding, J.; Welton, T.; Armstrong, D. W. *J. Am. Chem. Soc.* **2002**, *124*, 14247−14254.
(19) Jovanovski, V.; Orel, B.; Jerman, I.; Hočevar, S. B.; Ogorevc, B. *Electrochem. Commun.* **2007**, *9*, 2062−2066.
(20) Xiao, L.; Johnson, K. E. *J. Electrochem. Soc.* **2003**, *150*, E307−E311.
(21) Silvester, D. S.; Aldous, L.; Lagunas, M. C.; Hardacre, C.; Compton, R. G. *J. Phys. Chem. B* **2006**, *110*, 22035−22042.
(22) Allen, G. D.; Buzzeo, M. C.; Davies, I. G.; Villagrán, C.; Hardacre, C.; Compton, R. G. *J. Phys. Chem. B* **2004**, *108*, 16322−16327.
(23) Allen, G. D.; Buzzeo, M. C.; Villagrán, C.; Hardacre, C.; Compton, R. G. *J. Electroanal. Chem.* **2005**, *575*, 311−320.
(24) Zhang, J.; Zheng, J. B. *Electrochim. Acta* **2007**, *52*, 4082−4086.
(25) Anbar, M.; Meyerstein, D.; Neta, P. *J. Phys. Chem.* **1964**, *68*, 2967−2970.
(26) Neta, P.; Huie, R. E.; Ross, A. B. *J. Phys. Chem. Ref. Data* **1988**, *17*, 1027−1038.
(27) Kolthoff, I. M.; Coetzee, J. F. *J. Am. Chem. Soc.* **1957**, *79*, 1852−1858.
(28) Iwamoto, R. T. *Anal. Chem.* **1959**, *31*, 955.
(29) Popov, A. I.; Geske, D. H. *J. Am. Chem. Soc.* **1958**, *80*, 1340−1352.
(30) Zistler, M.; Wachter, P.; Wasserscheid, P.; Gerhard, D.; Hinsch, A.; Sastrawan, R.; Gores, H. J. *Electrochim. Acta* **2006**, *52*, 161−169.
(31) Aldous, L.; Silvester, D. S.; Villagrán, C.; Pitner, W. R.; Compton, R. G.; Lagunas, M. C.; Hardacre, C. *New J. Chem.* **2006**, *30*, 1576−1583.
(32) Silvester, D. S.; Broder, T. L.; Aldous, L.; Hardacre, C.; Crossley, A.; Compton, R. G. *Analyst* **2007**, *132*, 196−198.
(33) Rudolph, M.; Reddy, D. P.; Feldberg, S. W. *Anal. Chem.* **1994**, *66*, 589A-600A.
(34) MacFarlane, D. R.; Meakin, P.; Sun, J.; Amini, N.; Forsyth, M. *J. Phys. Chem. B* **1999**, *103*, 4164−4170.
(35) Schröder, U.; Wadhawan, J. D.; Compton, R. G.; Marken, F.; Suarez, P. A. Z.; Consorti, C. S.; de Souza, R. F.; Dupont, J. *New J. Chem.* **2000**, *24*, 1009−1015.
(36) Sharp, M. *Electrochim. Acta* **1983**, *28*, 301−308.
(37) Shoup, D.; Szabo, A. *J. Electroanal. Chem. Interfacial Electrochem.* **1982**, *140*, 237−245.
(38) Huddleston, J. G.; Visser, A. E.; Reichert, W. M.; Willauer, H. D.; Broker, G. A.; Rogers, R. D. *Green Chem.* **2001**, *3*, 156164.

(39) Hyde, M. E.; Compton, R. G. *J. Electroanal. Chem.* **2003**, *549*, 1−12.

(40) Broder, T. L.; Silvester, D. S.; Aldous, L.; Hardacre, C.; Crossley, A.; Compton, R. G. *New J. Chem.* **2007**, *31*, 966−972.

(41) Dunlop, P. J.; Stokes, R. H. *J. Am. Chem. Soc.* **1951**, *73*, 3456−3457.

(42) Noyes, R. M. *J. Phys. Chem.* **1965**, *69*, 3182−3183.

(43) Marassi, R.; Chambers, J. Q.; Mamantov, G. *J. Electroanal. Chem.* **1976**, *69*, 345−359.

(44) Weast, R. C., Ed. *Handbook of Chemistry and Physics*, 55th ed.; CRC Press: Boca Raton, FL,1974.

(45) Lide, D. R., Ed. *Handbook of Chemistry and Physics*, 76th ed.; CRC Press: Boca Raton, FL, 1996.

(46) Alden, J. A.; Hutchinson, F.; Compton, R. G. *J. Phys. Chem. B* **1997**, *101*, 949−958.

(47) Bard, A. J.; Faulkner, L. R. *Electrochemical Methods: Fundamentals and Applications*, 2nd ed.; Wiley: New York, 2001.